T.C.

BAHCESEHIR UNIVERSITY

GRADUATE SCHOOL

THE DEPARTMENT OF BIOENGINEERING

THE EFFECT OF GOLD NANOPARTICLES SYNTHESIZED BY GREEN SYNTHESIS METHOD ON GSK-3 BETA MRNA EXPRESSION IN HUMAN NEUROBLASTOMA CELL LINE

MASTER'S THESIS

FAWZI AL BAJOURY

ISTANBUL 2023

T.C.

BAHCESEHIR UNIVERSITY

GRADUATE SCHOOL

THE DEPARTMENT OF BIOENGINEERING

THE EFFECT OF GOLD NANOPARTICLES SYNTHESIZED BY GREEN SYNTHESIS METHOD ON GSK-3 BETA MRNA EXPRESSION IN HUMAN NEUROBLASTOMA CELL LINE

MASTER'S THESIS

FAWZI AL BAJOURY

THESIS ADVISOR

Assist. Prof. Dr. Canan Bağcı

ISTANBUL 2023

T.C.

BAHCESEHIR UNIVERSITY GRADUATE SCHOOL

...../...../.....

MASTER THESIS APPROVAL FORM

Program Name:	BIOENGINEERING (ENGLISH, THESIS)
Student's Name and Surname:	FAWZI AL BAJOURY
Name Of the Thesis:	**The Effect of Gold Nanoparticles Synthesized by Green Synthesis Method on GSK-3 beta mRNA expression in human neuroblastoma cell line**
Thesis Defense Date:	22/12/2023

This thesis has been approved by the Graduate School which has fulfilled the necessary conditions as Master thesis.

……..

Institute Director

This thesis was read by us, quality and content as a master's thesis has been seen and accepted as sufficient.

	Title/Name	**Signature**
Thesis Advisor's	Assist. Prof. Dr. Canan Bagci	
Member's	Assist. Prof. Dr. Mehmet Ozansoy	
Member's	Assist. Prof. Dr. Deniz Sezlev Bilecen	

I hereby declare that all information in this document has been obtained and presented in accordance with academic rules and ethical conduct. I also declare that, as required by these rules and conduct, I have fully cited and referenced all material and results that are not original to this work.

Name, Last Name: FAWZI AL BAJOURY

Signature:

ABSTRACT

THE EFFECT OF GOLD NANOPARTICLES SYNTHESIZED BY GREEN SYNTHESIS METHOD ON GSK-3 BETA MRNA EXPRESSION IN HUMAN NEUROBLASTOMA CELL LINE

Fawzi Al Bajoury

Biogenetic Engineering Master's Program

Supervisor: Assist. Prof. Dr. Canan Bağcı

December 2023, 31 Pages

As nanotechnology is one of the most promising era of many fields such as electronic field power field and health care and medicine field as many other field. In-depth research and biomedical applications such as genomics, biosensors, immunoassays, clinical chemistry, laser phototherapy of cancer cells and tumours, targeted drug delivery of drugs, DNA and antigens, optical bio imaging, and the monitoring of cells and tissues with the use of cutting edge detection systems, are all focused on gold nanoparticles with controlled geometrical and optical properties.

Plant generated AuNPs represent a great opportunity to be used in many field especially the medical field such as drug delivery and therapy, which those nanoparticles synthesised by green synthesis have a high antioxidant and anti-inflammatory quality as well their permeability that they can cross many biological barriers such as blood brain barrier, which is a very specific and selective barrier as it protect the brain from the foreign molecules, as well control what can pass and what couldn't to the central nervous system. Thus, they can be used for drug delivery in many neurodegenerative diseases. As signalling and metabolic enzyme, glycogen synthase kinase 3 beta (GSK-3β) participate in a number of biological functions, including signalling, cell cycle regulation, DNA repair and proliferation of cells. Many disorders such as cancer, diabetes, neurological disease, and inflammation have been linked to GSK-3 beta.

The primary objective of this study was be to examine the effect of gold nanoparticles produced by the green synthesis method on the expression of mRNA of GSK3β in SH-SY5Y human neuroblastoma cell line. We used both MTT and qPCR to see the effect of the gold nanoparticles on the gene express of GSK3β as well its toxicity on our cells and observe the ideal concentration of gold nanoparticle in terms of its biocompatibility. As a result, 10 μg/μl AuNPs was shown to be the most biocompatible concentration in SH-SY5Y human neuroblastoma cell and this concentration of AuNP increase the gene expression of GSK3β.

Keywords: Gold Nanoparticles, Green Synthesis, mRNA expression, GSK3-β

ÖZ

YEŞIL SENTEZ YÖNTEMIYLE SENTEZLENEN ALTIN NANOPARTIKÜLLERIN İNSAN NÖROBLASTOMA HÜCRE HATTINDA GSK-3 BETA MRNA EKSPRESYONUNA ETKISI

Fawzi AL BAJOURY
Biyomühendislik Yüksek Lisans Programı
Tez Danışman: Dr. Öğr. Üyesi Canan Bağcı
Eylül 2023, 31 sayfa

Nanoteknoloji, elektronik, sağlık ve tıp alanı gibi birçok uygulama alanda en umut verici yöntemlerin başında gelmektedir. Genomik, biyosensör, immünoanaliz, klinik kimya, kanser hücreleri ve tümörlerin lazer fototerapisi, ilaçların, DNA ve antijenlerin hedefe yönelik ilaç dağıtımı, optik biyo görüntüleme ve hücre ve dokuların kullanımıyla izlenmesi gibi derinlemesine araştırma ve biyomedikal uygulamalarda kullanılabilmektedir. Son teknoloji tespit sistemlerinin tümü, kontrollü geometrik ve optik özelliklere sahip altın nanoparçacıklarına odaklanmıştır.

Yeşil sentez yöntemiyle sentezlenen altın nanoparçacıklarının yüksek antioksidan ve anti-inflamatuar özelliğe sahip olmasının yanı sıra birçok biyolojik bariyeri geçebilecek özelliklere sahip olduğu ilaç taşıyıcılığı ve tedavi gibi tıp alanı başta olmak üzere birçok alanda kullanım için büyük bir fırsat sunmaktadır. Oldukça spesifik ve seçici bir bariyer olan kan beyin bariyeri merkezi sinir sistemine hangi moleküllerin geçip geçemeyeceğini kontrol eder. Böylece birçok nörodejeneratif hastalıkta ilaç taşıyıcı olarak kullanılabilirler. Metabolik bir enzim olan glikojen sentaz kinaz 3 beta (GSK-3β), hücre döngüsü düzenlemesi, DNA onarımı ve hücrelerin çoğalması dahil olmak üzere bir dizi biyolojik fonksiyona katılır. Kanser, diyabet, nörolojik hastalık ve inflamasyon gibi birçok bozukluk GSK-3 beta ile ilişkilendirilmiştir.

Bu çalışmanın temel amacı yeşil sentez yöntemiyle üretilen altın nanoparçacıklarının SH-SY5Y insan nöroblastoma hücre hattında GSK3β mRNA'sının ekspresyonu üzerindeki etkisini incelemektir. Altın nanoparçacıkların GSK3β'nın gen ekspresyonu üzerindeki etkisini ve hücreler üzerindeki toksisitesini görmek ve biyouyumluluk açısından altın nanopartikülünün ideal konsantrasyonunu gözlemlemek

için MTT ve qPCR analizleri yapıldı. Sonuç olarak, 10 µg/µl AuNP'lerin SH-SY5Y insan nöroblastoma hücresinde en biyouyumlu doz olduğu ve bu AuNP konsantrasyonunun GSK3β'nın gen ekspresyonunu arttırdığı gösterildi.
Anahtar Kelimeler: Altın nanoparçacıkları, Yeşil sentez, mRNA ekspresyonu, GSK3-β

To my beloved and caring family,

ACKNOWLEDGEMENTS

I would like to thank my supervisor, Assist. Prof. Dr. Canan Bağcı, for her direction, counsel, encouragement, and insight during the project. I'd want to express my gratitude to all of the doctors who taught me during my trip in Bahçeşehir University. Especially I would like to thank my thesis jury, Assist. Prof. Dr. Deniz Sezlev Bilecen and Assist. Prof. Dr. Mehmet Ozansoy. Also, special thanks to my colleagues Mohammed Dabbour, Wafaa and Asia.

And my father mohammed al bajoury and my mom jinan attieh.and my sisters iman and dima and my best frıend moeman for supporting me during my thesis.

And I would like to thanks my advisor again for being supportive and being so understanding no matter how much we struggle.

TABLE OF CONTENTS

LIST OF FIGURES

LIST OF TABLES

LIST OF ABBREVIATIONS

APP	Amyloid Precursor Protein
AuNPs	Gold Nanoparticles
Aβ	Amyloid beta
Bay leaves	Laurus nobilis
BBB	Blood-Brain Barrier
CNS	Central Nervous System
CSF	Cerebrospinal Fluid
DMSO	Dimethyl sulfoxide
FT-IR	Fourier Transform Infrared Spectroscopy
$HAuCl_4$	Chloroauric acid
NFTs	Neurofibrillary Tangles
NH_4OH	Ammonium hydroxide
NPs	Nanoparticles
SEM	Scanning Electron Microscope
Tau	Hyper phosphorylated Protein
UV	Ultraviolet Visible Spectroscopy

XRD	X-ray diffraction

Chapter 1

Introduction

Glycogen synthase kinase 3 (GSK3) is a proline-directed serine/threonine kinase that is constitutively active and involved in a variety of physiological pathways from glycogen metabolism to gene transcription. GSK3 also plays a significant and central role in the pathogenesis of Alzheimer's disease (AD), prompting us to coin the phrase "GSK3 hypothesis of AD." According to this theory, GSK3 hyperactivity is responsible for memory impairment, hyperphosphorylation of tau protein, elevated amyloid production, and local plaque-associated inflammatory responses mediated by microglia. Multifunctional serine/threonine kinase GSK3β is responsible for several metabolic processes, specifically in the developing central nervous system (CNS) (Hooper et al.,2008).

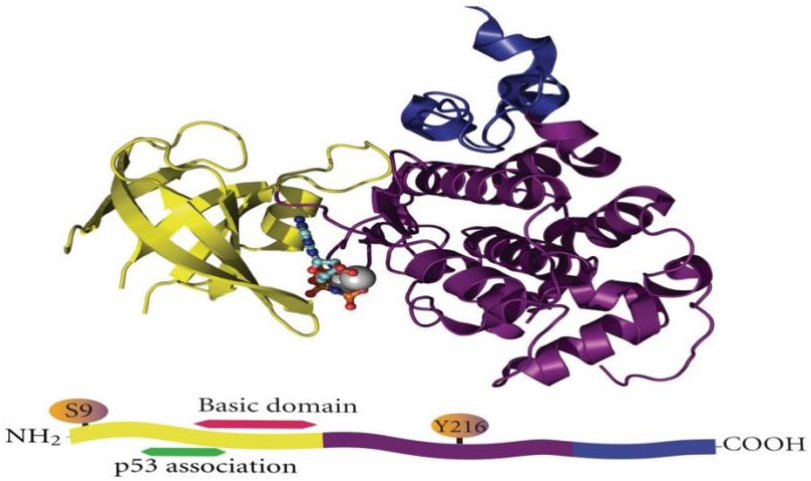

***Figure 1**: Glycogen synthase kinase-3β (GSK-3β) structure*

Because GSK3β has a wide range of substrates, including transcription factors, structural proteins, and metabolic/signalling proteins, it plays a key role in a number of developmental processes in the developing brain, including neurogenesis, neuronal migration, differentiation, and survival. Developmentally controlled, GSK3β activity is affected by a range of environmental and cellular stressors, including oxidative stress, endoplasmic reticulum stress, and nutritional/trophic factor deficiency. GSK3β activity anomalies may interfere with CNS development. Thus, GSK3β is an essential signalling protein that controls the development of the brain. Additionally, it could ascertain how

vulnerable neurons are to harm from different environmental assaults (Phukan et al., 2010).

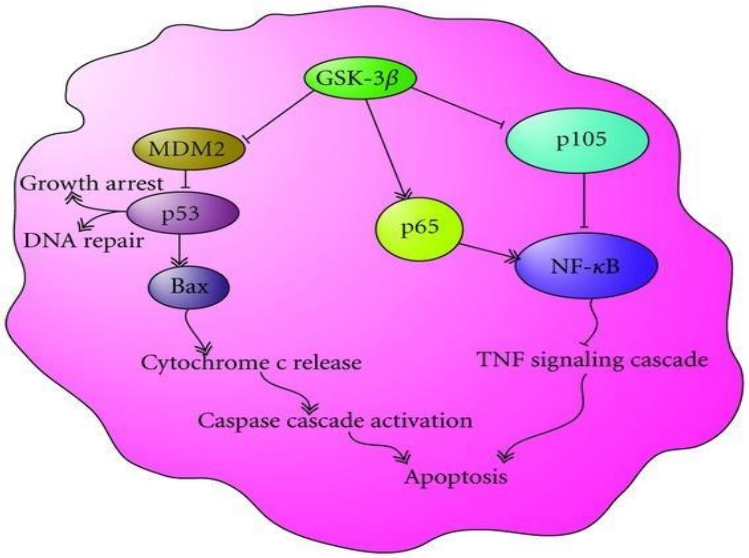

Figure 2*: The role of GSK-3β in apoptosis signalling. The diagram shows the role of activated GSK-3β and its role in apoptosis regulation. Active GSK-3β inhibits MDM2 regulation of p53, resultin in DNA repair and growth arrest. Moreover, in some cases caspase cascade activation via Bax promotes apoptosis. Active GSK-3β positively regulates NFκB by activating IKK, IκB, and p65, resulting in the inhibition of apoptosis mediated by TNF's. These mechanisms are responsible for the inhibition of apoptosis initiation via TNF signalling cascade.*

The vascular structure known as the blood-brain barrier (BBB) divides the central nervous system (CNS) from the rest of the circulatory system. Apart from its function as a barrier, the blood-brain interface actively controls the inflow and outflow of chemicals. BBB efficiently controls the flow of molecules and ions, delivering vital nutrients and oxygen to neurons in response to their immediate needs. Furthermore, it serves as a shield against pathogens and potentially harmful substances, creating an environment that is ideal for neural function (Obermeier et al., 2013). An increasing amount of evidence indicates that aging, cerebrovascular injury, accumulation, and/or other factors may affect multiple components of the neurovascular unit, which may ultimately result in BBB dysregulation When the BBB is disrupted, it affects neurons, which makes it more difficult for amyloid-beta to be cleared in the neurovascular unit.

Thus, it is anticipated that this will create a detrimental feedback loop between the accumulation of Aβ and the BBB's dysfunction throughout AD development (Yamazaki & Kanekiyo, 2017).

Nanotechnology is broadly perceived as a promising innovation for various applications. It empowers specialists to appreciate and control materials at the nuclear and sub-atomic level. Nanotechnology utilizes substances or parts that display the most negligible working design at the nanometre scale, which ranges from 1 to 100 nm. Nanoparticles (NPs) may be intended to connect with natural particles or ligands that are capable of address labels, working with the designated conveyance of NPs to determined areas in the body (Gupta et al., 2019, Safari and Zarnegar, 2014). The formation of biomolecules to nanoparticles offers a different cluster of uses across different disciplines, including detecting, imaging, conveyance, catalysis, and treatment. Gold NPs (AuNPs), which are among frequently studied and used NPs, can really organize numerous biomolecules, working with their assembling and alteration to control the construction and action of such biomolecules, outperforming the abilities of option nanoparticles. In addition, AuNPs exhibit a similar size range as proteins and may be intentionally modified to possess a surface that closely mimics biological structures. The nanopeptide, comprising of bioactive peptides immobilized on gold nanoparticles, is viewed as an entirely helpful specialist with added usefulness. The outer layer of bound round nanoparticles can upgrade the bioactivity of peptides through exceptional synergistic impacts (Zhang et al., 2021).

The aim of this thesis study is to examine the impact of AuNPs, manufactured using a green synthesis method, on the expression GSK3β mRNA in SH-SY5Y human neuroblastoma cell line.

Chapter 2

Literature Review

2.1 GSK3beta and its importance in the cell

In quiescent cells, GSK3β is constitutively active and responds to various environmental stimuli (Grimes & Jope, 2001; Grimes and Jope, 2001; Doble and Woodgett, 2003). Phosphorylation at specific sites controls GSK3β activity. Tyrosine 216 (Tyr216) phosphorylation is usually necessary for fully-functioning GSK3β, but serine 9 (Ser9) phosphorylation reduces GSK3β activity. Most often occurring and significant regulating mechanism is Ser9 phosphorylation. Numerous kinases, such as p70 S6 kinase, extracellular signal-regulated kinases (ERKs), p90Rsk (also known as MAP-KAP kinase-1), protein kinase B (also known as Akt), specific isoforms of protein kinase C (PKC), and cyclic AMP-dependent protein kinase (protein kinase A, PKA), are able to phosphorylate Ser9 (Grimes and Jope, 2001; Kaytor and Orr, 2002).

Tyrosine phosphorylation of GSK3β boosts the enzyme's activity in contrast to the inhibitory regulation of the enzyme that occurs via serine phosphorylation. There are not many studies on GSK3β tyrosine phosphorylation. Proline-rich tyrosine kinase 2 (PYK2), a calcium-dependent tyrosine kinase, and/or Fyn, a member of the Src tyrosine family, are reported to be the mediators of pGSK3β (Tyr216) stimulation (Bhat et al., 2000; Hartigan & Johnson, 1999); Lesort et al., 1999; Sayas et al., 2006). Mitogen-activated protein kinase kinase (MEK1/2) regulates pGSK3β (Tyr216), as well (Takahashi-Yanaga et al., 2004). It has been proposed that autophosphorylation controls GSK3β tyrosine phosphorylation (Cole et al., 2004).

Tyr216 and Ser9 phosphorylation appears to be unchanged when GSK3β is active (Baltzis et al., 2007). GSK3β's subcellular location may potentially play a role in its regulation. While some of GSK3β's substrates, like Tau, are cytosolic, others—most notably, a number of transcription factors—are nuclear. Therefore, for GSK3β to control these proteins, it has to be present in both compartments. According to Diehl et al. (1998), nuclear GSK3β increases throughout the cell cycle's S phase. Tyr216phosphorylated GSK3β translocates to the nucleus in response to proapoptotic stimuli (Bhat et al., 2000). The processes behind the transition of GSK3β between the

cytosolic and nuclear compartments were clarified by the discovery of a nuclear localization sequence (NLS) in the protein (Meares & Jope, 2007)

Despite being extensively expressed in every tissue, GSK3β is most prevalent in the central nervous system (CNS) (Woodgett, 1990) GSK3β is mostly expressed in neurons and hardly noticeable in astrocytes in the developing brain (Leroy & Brion, 1999; Takahashi-Yanaga et al., 2004) According to Leroy and Brion (1999), GSK3β is most expressed in the developing rat brain between the ages of 18 days during embryonic life and 10 days during postnatal life (PD10). Subsequently, the expression diminishes and reaches its minimum in adults; robust GSK3β immunoreactivity is restricted to growing neurons, with relatively moderate detection in neuroblast-containing layers. GSK3β is found in the proximal portion of dendrites and perikarya both throughout development and in adults.

Axonal tracts in the embryo also have a strong GSK3β positivity. By PD10, this axonal immunoreactivity has significantly diminished, and by PD20, it is completely eliminated in adults (Leroy & Brion, 1999) Similarly, Takahashi et al. (2000) demonstrate that during the first two weeks after birth, GSK3β expression was high in the rat brain and the levels reach to peak at PD8–11 while its expression dramatically drops by PD20. Coyle-Rink and colleagues (2002) investigate GSK3β expression in the growing mouse brain. Similar to the rat brain, the mouse brain has robust GSK3β expression in the first two postnatal weeks, followed by a sharp decline in GSK3β levels after PPD18.

2.1.1 Correlation between GSK3β and central neuroinflammatory diseases

One important process linked to a number of neurological disorders is neuroinflammation. Recent research has demonstrated that GSK3β dysregulation regulates the mechanisms involved in neuroinflammation, which in turn plays a role in the onset and progression of various diseases. GSK3β inhibitors have demonstrated advantages in several neuroinflammatory disease models, such as Alzheimer's disease and multiple sclerosis. (Draz & Shafiee, 2018).

2.2 The blood-brain barrier

The blood–brain barrier (BBB) is the microvasculature and a significant barrier to protect the brain in central nervous system (CNS). CNS vessels contain an arrangement

of additional characteristics that allow them to strictly control the transporation of particles, and cells between the blood and the CNS (Zlokovic, 2008; Daneman, 2012). This intensely confining boundary capacity permits BBB ECs to firmly direct CNS homeostasis, which is basic to permit for appropriate neuronal work, as well as ensure the CNS from poisons, pathogens, irritation, damage, and illness. The prohibitive nature of the BBB gives a deterrent for medicate conveyance to the CNS, and, in this way, major endeavours have been made to create strategies to tweak or bypass the BBB for conveyance of therapeutics (Larsen et al., 2014). Disruption of these boundary properties lead to neurological disorders such as stroke, multiple sclerosis, brain injuries, and neurodegenerative disorders, could be a major component of the pathology and movement of these infections (Zlokovic, 2008; Daneman, 2012). BBB disruption can lead to metabolic dysregulation, altered signalling homeostasis leading to neuronal disruption and degeneration.

In spite of the fact that key properties of the BBB are shown inside the ECs, imperative transplantation considers have appeared that they are directed by intuitive with the microenvironment of the CNS (Stewart & Wiley, 1981; Janzer & Raff, 1987). Disturbance of the BBB is investigated in numerous diverse neurological disorders counting MS, stroke, Alzheimer's disease, epilepsy, and traumatic brain injuries. Imaging of human patients and examination of post-mortem brain analyses has distinguished the obsessive breakdown of the obstruction totally different neurological infections. In expansion, work with model organisms of infection and with cell culture BBB models has empowered the distinguishing proof of a few of the molecular components that cause changes to the BBB. This disruption can incorporate modifications in numerous diverse properties of the BBB counting TJs, transporters, transcytosis, and LAM expression. This breakdown can lead to edema, disturbance of ionic homeostasis and changed signalling that can lead to neuronal dysregulation and, eventually, degeneration (Moyaert et al., 2023).

The BBB is an essential cellular boundary that firmly controls the microenvironment of the CNS to permit for normal neuronal function. This obstruction is a critical to factor when deciding medicines for diverse neurological disorders, both since disturbance of the BBB can lead to extreme pathology watched in numerous diverse infections. BBB is a fundamental consideration within the advancement of CNS-acting therapeutics. Later work has distinguished numerous particles required for BBB

work as well as numerous of the cellular and molecular signalling pathways that direct the arrangement of the BBB amid advancement, its work in adulthood, and its reaction to affect and infection (Figure 3) (Daneman & Prat, 2015).

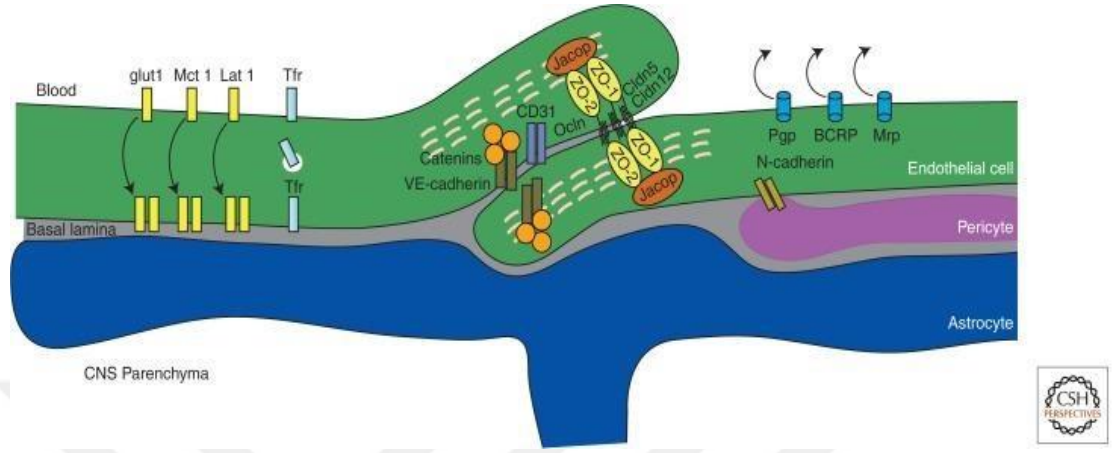

Figure 3*: Schematic representation of various molecules and proteins in BBB (Daneman & Prat, 2015).*

In spite of the fact that much advance has been made, numerous questions are to be elucidated. Are all of the distinctive characteristics of the BBB directed by the same pathways or distinctive pathways? How are diverse signalling pathways facilitated to direct distinctive viewpoints of the BBB? Are diverse BBB properties, counting the transport and tight intersections, powerfully controlled in reaction to neural activity? How do modifications within the BBB influence neuronal movement, brain work, and behaviour? What leads to disruption of BBB properties due to neurological disorder? Understanding these questions will permit for the improvement of therapeutics to balance the BBB both to re-establish its function for neurological infection and to create strategies to bypass the BBB for medicate conveyance (Figure 4) (Daneman & Prat, 2015).

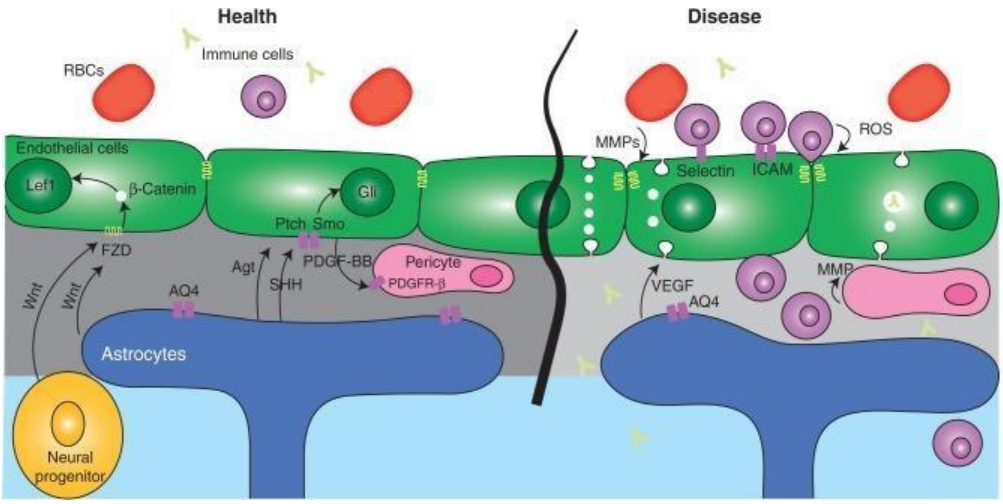

***Figure 4**: Schematic representation of signalling molecules regulating the BBB in healthy and disease states. ICAM, intercellular adhesion molecule; MMP, matrix metalloproteinase; ROS, reactive oxygen species (Daneman & Prat, 2015).*

2.3 Nanoparticles

A nanoparticle has a diameter size range between 1 to 100 nanometres. Nanoparticles can show distinctive physical and chemical properties when compared to their bulk counterparts. The particle properties are changed as their estimate approaches the nuclear scale. This is often due to the surface area to volume proportion expanding, coming about within the material's surface molecules ruling the material execution. The superior properties enable nanoparticles to have various optical, physical and chemical properties, as they restrict their electrons and create quantum impacts (https://www.twi-global.com/technical-knowledge/faqs/what-arenanoparticles).

Nanomaterials can be produced, be made as the by-products of combustion reactions, or be created intentionally through designing to perform a particular work. Due to the capacity to synthesize the materials in a specific way, the utilization of nanomaterials ranges over a wide applications, from healthcare and beauty care products to natural conservation and environmental decontamination (Adib Bin Rashid., 2023).

Carbon nanotubes are being synthesized in arrange to be utilized in forms such as the attachment of antibodies to the nanotubes to form biosensors. In aviation, carbon nanotubes can be utilized within the morphing of flying machine wings. The nanotubes are utilized in a composite shape to twist in reaction to the application of an electric voltage. Natural conservation forms make utilize of nanomaterials as well - in this case, nanowires. Applications are being created to utilize the nanowires - zinc oxide

nanowires- in adaptable sun-oriented cells as well as to play a part within the treatment of contaminated water (Malik et al., 2023). Within the makeup industry, nanoparticles – such as titanium oxide – are utilized in sunscreen, due to their improved stability. Titanium oxide nanoparticles are able to supply progressed UV protection whereas too having the included advantage of evacuating the cosmetically unappealing brightening related with sunscreen in their nanoform (Smijs & Pavel, 2011). The utilization of nano-titanium dioxide, moreover, expands to be used in coatings to make self-cleaning surfaces, such as those of plastic cultivate chairs (Smijs & Pavel, 2011). Controlling the size, shape and properties of the nanoparticle empowers engineers to plan photovoltaics and sun based warm items with custom fitted sun-oriented assimilation rates (Smijs & Pavel, 2011).

One of the most important application of nanoparticles is in the medical field to mediate the delivery of chemotherapy drugs specifically to cancerous tissues. The nanoparticles are compelling for drug delivery because they can exceptionally accurately discover unhealthy cells and deliver the medication to damaged tissues. This implies that one can suffice with less dose and less side effects. In expansion, nanoscience and nanotechnological strategies are impelling the advancement of more advanced instruments for identifying diseases, such as cancer and atherosclerosis, at early stages and performing neurosurgery. Furthermore, applications of nanotechnology in diagnosis of diseases are studied (Yusuf et al., 2023).

2.4.1 Gold Nanoparticles

Because of their intriguing optical properties for imaging and detection, biocompatibility, ease of biological production, potential ability to cross the blood brain barrier, and low toxicity, AuNPs have drawn interest from a variety of nanoparticles (Bilal et al., 2020). Compared to 18 nm gold nanoparticles, which exhibit very strong cellular and nuclear penetration, AuNPs with a length of 1 nm can interact with DNA by passing through the cell membrane and reaching to nucleus (Khan et al., 2014; Kong et al., 2017). Because AuNPs naturally contain anti-inflammatory and antioxidant properties that may be used to treat neurodegenerative diseases, they hold great promise for the treatment of neurodegenerative disorders such as AD. Additionally, AuNPs in the brain stimulate glial cells and mute macrophages (dos Santos Tramontin et al., 2020). The elimination from the body might be via clearance through the reticuloendothelial

system (RES) within the circulation or circulated for a long-term depending on the shape, size, and surface properties of the nanoparticle (Hammami et al., 2021). The physical and chemical characteristics of AuNPs make them suitable for a range of uses in the disciplines of stimulation, biological labelling, detection and diagnostics, drug transport and treatments, and biological labelling. According to Elahi et al. (2018), AuNPs' form, optoelectronic characteristics, and notable surface-to-volume ratio make them essential tools in the biotechnology industry. Specifically, passive diffusion or active energy-based delivery methods are used as the medium via which AuNPs are delivered. When AuNPs are taken orally, they enter the body through the digestive tract and are mostly distributed through the venous system. Furthermore, they might be immediately delivered intravenously to the desired organs. Two methods might be used to synthesise AuNPs: "top-down" (physical manipulation) and "bottom-up" (chemical shift). The production of AuNPs, which are experts at regulating their size, shape, stability, solubility, and functionalities, has required a great deal of work. The biological method, which uses plants, algae, and fungi, offers a way around these problems. There are many ways to synthesize NPs, including physical and chemical approaches. However, these methods have drawbacks in terms of the toxic by-products utilized or high energy requirements. Due to the major advantages it offers in terms of both the environment and economy, biosynthesis of NPs has garnered a lot of attention lately. Plants have shown a great deal of promise as practical options for producing NPs. Compared to microorganism-derived nanoparticles, plant-derived nanoparticles are more stable and synthesise at a faster pace (**Mikhailova EO.,** 2021).

By delivering the drug or therapeutic molecules to target cells, nanotechnology has demonstrated a high degree of ability to treat a variety of diseases. It has also overcome many of the challenges faced by traditional treatments, including BBB passage, decreased digestive system efficacy, shorter half-lives, and quick excretory system medication elimination. Furthermore, large quantities required for conventional therapies have detrimental consequences on the body (Karthivashan et al., 2018).

When AuNP-loaded therapies are applied to cells, passive or active targeting mechanisms are employed. Larger molecules are able to pass through the endothelium by passively targeting its EPR when AuNPs concentrate within the tumour due to an uneven blood vessel microenvironment (Yeh et al., 2012).

AuNPs have several advantages over other nano carriers in drug delivery systems, such as their special optical, chemical-physical, and biocompatible properties. Functional flexibility, the capacity to alter monolayers, controlled dispersion, stability, a sizable surface area for drug loading, and non-toxicity are the main characteristics covered in this context. Small interfering RNAs (siRNAs), proteins, peptides, plasmid DNA, and other chemotherapeutic agents can all be successfully transported by means of their tiny carriers (Elahi et al., 2018).

Because AuNPs are needed in small amounts, they are inexpensive and extremely effective diagnostic tools that have transformed the medical diagnostics industry. Early diagnosis contributes to more affordable and successful therapy. Due to its low cost, great sensitivity, speed, accuracy, and minimal symptoms of a wide range of disorders, AuNPs have garnered a lot of interest (Kalimuthu et al., 2020).

Numerous nanosensor-based diagnostic methods have been developed and proven effective as biomarkers for AD diagnosis. Porous magnetic microspheres (PMM) are a useful platform for gathering and pre-concentrating AD biomarkers. PMMs help to fix antibodies to the surface of particles, which enhances the effectiveness of obtaining AD/biomarker analyses from human blood samples. High-performance PMMs after the contact increase AuNPs' catalytic activity, and the ensuing electrocatalytic tags are useful for analyte detection (Ramamurthy et al., 2013).

Surface plasmon resonance with localization (LSPR) and surface-enhanced Raman scattering (SERS) are essential tools in the diagnostics sector. Spectrum modulation is the reason behind the use of AuNPs in LSPR-based applications. In the realm of diagnostics, the localised surface plasmon resonance (LSPR) phenomenon that results from AuNPs absorbing photon energy is highly significant. SERS is another incredibly attractive spectroscopic method utilised in diagnostics because of its high sensitivity and non-invasive nature (Hu et al., 2020).

Chapter 3

Methodology

3.1 Chemicals

Laurus nobilis, or bay leaves, from Istanbul, Turkey's market. 99.9% ethanol (Isolab). Powdered hydrochloroauric acid (HAuCl4) (Sigma Aldrich, St. Louis, Missouri, USA). Heat-Inactivated Foetal Bovine Serum (HI FBS) is available from Gibco, UK. Modified Eagle Medium (DMEM) produced by Dulbecco (Gibco, United Kingdom). Trypan Blue Stain (0.4%) from Gibco (UK) Inc. Ammonium hydroxide 25% (NH_4OH) and dimethyl sulfoxide (DMSO) are sold by Sigma Aldrich in St. Louis, Missouri, in the United States. 10,000 U/mL Penicillin-Streptomycin (PAN-Biotech, United Kingdom). Aβ, or beta-amyloid peptide (1-42) (Abcam, UK).

3.2 Gold Nanoparticle Biosynthesis

3.2.1 Extract Preparation

The fresh bay leaves were bought from the market. Before being used, the leaves were repeatedly rinsed with deionized water to get rid of any last bits of dust. The plants were allowed to air-dry before being ground into a powder in a coffee grinder and then filtered through a 0.5 mm mesh screen to guarantee uniform size. In an Erlenmeyer flask, around 20 g of the powdered leaves were combined with 100 mL of distilled water to create a 20% (w/v) solution. After an hour of magnetic stirring and heating to 76 °C, the solution was allowed to cool. Following the extraction, the extract was allowed to cool to room temperature using filter paper. The filtered material was kept cold, 4°C, until it was needed.

3.2.2 Gold Nanoparticles Biosynthesis

For two hours, a 15 mL extract made from bay leaves was used to reduce a 90 mL aqueous solution containing 1 mM of auric acid ($HAuCl_4$) at ambient conditions. A pink-red solution was the end product, indicating that the synthesis of gold (AuNPs) was successful. The mixture was centrifuged twice for 20 minutes at 4000 rpm, and the supernatant was discarded. To remove any biomolecules that hadn't reacted, the

fragment containing the AuNPs was centrifuged at 15,000 rpm for 6 minutes after being treated to 3 washes with 99.9% ethanol. An accurate marker of the successful synthesis of AuNPs was the reaction mixture's observed shift from a brown-yellow to a purple colour.3.3Gold nano particle characterization

3.3 Characterization of AuNPs

3.3.1 Ultraviolet Visible Spectroscopy

One of the frequently used analytical method for determining light transmittance or absorbance is UV-visible spectroscopy. Although the visible spectrum extends up to 800 nm and the UV wavelength runs from 100 to 380 nm, it is important to remember that most spectrophotometers work within a wavelength range of 200 to 1100 nm. Matter's chromatic characteristics, or colour, are largely determined by the process by which it absorbs and releases light (Rocha et al., 2018). UV-visible spectroscopy is frequently used in nanomaterial investigation to determine the formation of nanoparticles. In nanoparticle research, UV-visible spectroscopy is often used in conjunction with affinity labelling to evaluate the reaction. It was suggested that by using a fitting process that fits the location of surface Plasmon resonance (SPR) with a straightforward wavelength functional, it may be possible to deduce the size dispersion of nanomaterials from their optical properties (C. Martínez et al., 2013). A

1 mL amount of AuNPs solution is added to the cuvette, and a wavelength span of 200–800 nm is used for the measurement.

3.3.2 X-Ray Diffraction

A highly effective non-destructive technique for characterizing materials having crystalline structure is XRD. The information provided includes details about a variety of topics, including phases, favoured crystalline additional structural characteristics, and orientations. The average grain size, crystallization, strain, and crystal deficiencies are some of these other characteristics. Constructive interference is the result of a monochromatic X-ray beam scattering at specified angles across several sets of lattice planes inside a given material. This interference produces X-ray diffraction peaks. The way the particles are arranged in space within the lattice determines the peak intensity.

As a result, the periodic atomic structures contained in a particular substance may be uniquely identified by the X-ray diffraction pattern (Bunaciu et albe2015).

3.3.3 Scanning electron microscopy (SEM)

SEM is a very versatile and advanced instrument that is commonly used to observe surface phenomena in a variety of materials. Using high-energy electrons, the specimen is analysed in a scanning electron microscope (SEM), and the released electrons and X-rays are then examined. The X-rays and electrons that are released give important information on a material's composition, topography, morphology, grain orientation, and crystallographic features. Morphology is the study of an object's physical characteristics, such as its size and form. On the other hand, topography describes the surface properties of that object, including its texture, look, and level of smoothness or roughness. In the same way, composition describes the components and compounds that make up a substance, while crystallography deals with the arrangement and structure of atoms inside those materials. The majority agreed that the scanning electron microscope (SEM) is the best tool for creating incredibly detailed visual representations of particles. Achieving remarkable 1 nm spatial resolution. Up to 300,000 times magnification is possible with this particular gadget. Scanning electron microscopy (SEM) is still a useful instrument for analysing the crystallographic, magnetic, and electrical characteristics of materials, despite its limitations in revealing interior information. Furthermore, SEM may be used to evaluate how surface changes with other molecules have affected the morphology of particles (Akhtar et al., 2018).

3.4 Cell culture

SH-SY5Y cells were cultured cell in Dullbecco's Modified Eagle Medium (DMEM) (Gibco, Germany) supplemented with 10% fetal bovine serum [FBS] (Gibco, Germany) and 100 g/ml penicillin/streptomycin (Gibco, Germany). These plates were incubated at 37°C and 5% CO_2 and the medium was replaced with the fresh medium within two days. For the subculture procedure, the attached cells were administered with 0.05% trypsin EDTA (Gibco, Germany) and incubated at 37°C for 5 minutes. They were collected by centrifugation at 1500x*g* for 5 min. SH-SY5Y cells were cultured in T25

cell culture flasks as 500.000 cells / T25 flask. They were incubated overnight at 37°C and 5% CO_2.

3.5 MTT

The main goal of the MTT (3-[4,5-dimethylthiazol-2-yl]-2,5 diphenyl tetrazolium bromide) test is to relatively efficiently quantify the presence of live cells without necessitating sophisticated cell counting processes. Therefore, the main use is evaluating the cytotoxic effects of different medications at different dosages. The MTT test principle deepens on the fact that live cells' mitochondrial activity. The tetrazolium salt MTT can be enzymatically converted into formazan crystals by living cells with mitochondrial activity. The crystals can then be dissolved to be measured by the optical density (OD) of formazan crystals by using a plate reader at wavelength of 570 nm (van Meerloo et al., 2011). 10,000 SH-SY5Y neuroblastoma cells were seeded into each well of a 96-well plate, with 100 µL of complete medium in each well to determine the biocompatible concentration of AuNPs. The cells were incubated for 24hour period, and 50 µL of AuNPs at concentrations of 10, 25, 50, and 100 µg/µl were administered to respective wells. 10% DMSO was used as the negative control and autoclaved dH_2O was added to the control group. After 24 hours of incubation, the cells were treated with DMSO and absorbance was measured at 570 nm.

3.6 RNA Isolation

10^6 SH-SY5Y cells were seeded to T75 flasks as 3 different groups; positive control, AuNP (10 µg/µl) treated group and DMSO treated group. After incubating for 24 hours, relative treatments were performed.

1 ml of Trizol was added to each T75 flasks and transferred to micro centrifuge tubes. Samples were vortexed and 200 µl of chloroform was added to each tube. After three minutes incubation at room temperature, the samples were centrifuged for 15 minutes at 4°C at 12,000 x g. Three layers were visible following the centrifugation: total RNA in the upper aqueous phase, proteins in the bottom layer, and DNA is in the interphase. The top aqueous phase was transferred to a fresh micro centrifuge tube without disrupting the interphase layer. 500 µl of isopropanol was added to each sample and they were incubated for 40 minutes at -20°C. At the end of incubation, the samples were centrifuged for 25 minutes at 4°C at 12,000 x g. After removing the supernatant, 1 millilitre of 75% ethanol was added to pellet. Then, samples were centrifuged at 7,500x

g for 5 minutes at 4°C. Ethanol was evaporated by air drying. Finally, RNA was dissolved 30 µl of autoclaved distilled water. To determine the concentration and purity of isolated RNA, Nano Drop spectrophotometer was employed.

3.7 cDNA Synthesis

cDNA synthesis from isolated total RNA was performed by using the One Script Plus cDNA Synthesis Kit (abm, Germany). After the RNA concentration measurement, the final RNA concentrations and volumes to be used in cDNA synthesis were adjusted to 1000 ng/ µl. The cDNA synthesis was performed according to the manufacturer's instructions. The volumes and the reagents that were used in cDNA synthesis reaction are shown in Table 1. When all mixtures were prepared, the samples were incubated at 55°C for 15 minutes and the reaction was terminated by incubating them at 85°C for 5 minutes.

Table 1

cDNA reaction mix

Reagent	Volume
5X RT Buffer	4 µl
dNTP	1 µl
Oligo dT primers	1 µl
Total RNA	1000 ng/ µl
OneScript® Plus RTase	1 µl
Nuclease free H_2O	4,67 µl

3.8 Primer Synthesis

The primers sequences were determined based on their NCBI accession numbers. The primer design was done as they bypass the introns, in the exon-exon spanning regions, preventing the amplification of any the contaminating DNA samples with intronic sequences. The selected primers are listed listed in Table 2 demonstrating the NCBI accession numbers, the primer sequences, the Tm values, and the distilled water volumes to prepare 100 µM stock primer solution. These primers were utilized for qPCR experiments. To prepare a 25 µM intermediate stock, 75 µl of dH_2O was added to 25 µl of 100 µM stock primer. For a 5 µM working primer solution, 80 µl of dH_2O were added

to 20 µl of 25 µM intermediate stock primer solution. All the qPCR experiments were performed by using 5µM working primer solution.

Table 2

The primer sequences of GAPDH and GSK3β

Gene name and NCBI accession number	**Sequence**	**Tm values**	**Distilled water added for 100µM stock**
GAPDH (NM_001289745.1) FP	5'-CAATGACCCCTTCATTGACC-3'	57°C	500 µl
GAPDH (NM_001289745.1) RP	5'-TTGATTTTGGAGGGATCTCG-3'	55°C	456 µl
GSK3 beta (NM_001146156.2) FP	5'-CTCAGGAGTGCGGGTCTTC-3'	61°C	410 µl
GSK3 beta (NM_001146156.2) RP	5'-AAGAGTGCAGGTGTGTCTCG-3'	59°C	509 µl

3.9 Quantitative Real Time Polymerase Chain Reaction (qRT-PCR)

qRT-PCR reactions were performed by using the Hot FirePOL EvaGreen qPCR Super mix (Solis Biodyne), according to the manufacturer's instructions. The reactions were run by the BioRad CFX96 Real Time System. Melting curves for each gene were analysed to show that specific amplicon replication was obtained. All reactions performed in duplicates for each biological replicate. Each reaction also included no template control.

The reactions were optimized for each primer and gene for the qRT-PCR reactions and the optimized reactions are shown at the following (Table 3-5).

Table 3

qPCR reaction mix

Component	Volume	Final concentration
HOT FIREPol® EvaGreen® qPCR Supermix (5x)	4 µl	1X
Forward primer (5 µM)	0,8 µl	200 nM
Reverse primer (5 µM)	0,8 µl	200 nM
cDNA template	2 µl	1 µg
H_2O	12,4 µl	up to 20 µl
TOTAL	20 µl	

Table 4

qPCR cycle protocol for GAPDH

Cycle step	Temperature	Time	Cycles
Initial activation	95°C	12 min	
Denaturation	95°C	15 sec	38
Annealing	58°C	30 sec	
Extension	72°C	30 sec	
Melting	50°C – 99°C		

Table 5

qPCR cycle protocol for GSK3β

Cycle step	Temperature	Time	Cycles
Initial activation	95°C	12 min	
Denaturation	95°C	15 sec	38
Annealing	58,3°C	30 sec	
Extension	72°C	30 sec	
Melting	50°C – 99°C		

After completing all qRT-PCR reactions, the threshold cycles (Cts) were determined for each sample. The relative expression levels of GSK3β relative to GAPDH (housekeeping gene) were calculated by using $2^{-\Delta\Delta Ct}$ method.

3.10 Statistical Analysis

The data are represented as mean ± SEM. Unpaired, two-tailed Student's t test was utilized for the MTT and mRNA expression analyses. $p<0.05$ was considered as statistically significant.

Chapter 4

Results and Discussion

4.1.1 Ultraviolet Visible Spectroscopy

When used to characterize metallic element nanoparticles (NPs), (UV-vis) spectroscopy appears to be very beneficial. Through examination of the particles' UV-vis spectroscopy, the production of AuNPs was confirmed. As seen in Figure 5, the measured solution features a surface plasmon band that is easily visible and is characterized by a broad absorption peak at 564 nm.

This phenomenon, which is a prominent characteristic of the gold surface Plasmon band and indicates the presence of AuNPs in the solution, results from the reduction of $HAuCl_4$ by bay leaf extract.

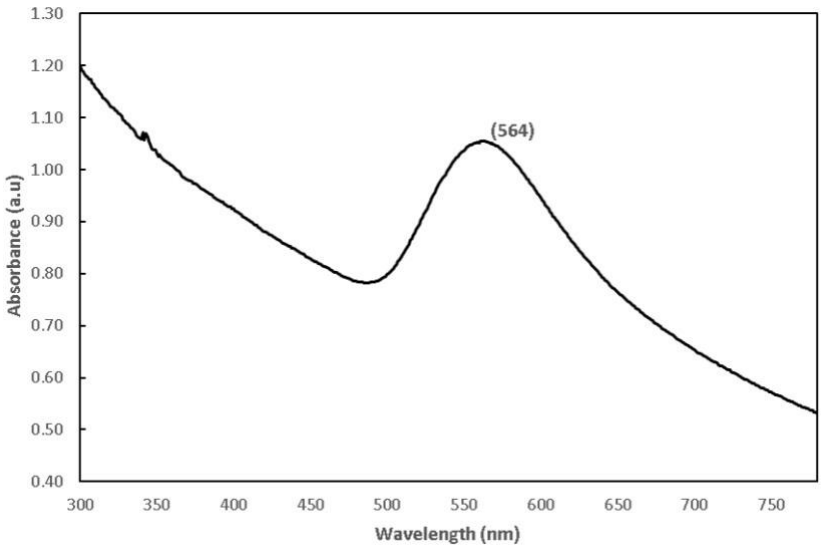

***Figure 5**: UV-visible spectroscopy of AuNPs*

4.1.2 X-Ray Diffraction

It was confirmed that the colloidal AuNPs were crystalline. Three unique peaks were seen at 44.8°, 52.1°, and 77.1° after bay leaf extracts were used to produce AuNPs (Figure 6). These peaks can be attributed to the (200), (200), and (311) crystallographic planes, respectively. The reflections from the face-centred cubic (FCC) phase of metallic

gold nanoparticles are indicated by the measured intensities. The resultant data provide strong proof that the AuNPs produced by using extracts from bay leaves have a crystalline structure. Using Debye-Scherrer's equation (formula 1), the mean diameter of the many particles was found to be 65.4 nm.

$D = K\lambda\beta \cos\theta$ (1)

Formula 1. Debye-Scherrer's equation.

K, the shape-dependent Scherrer's constant, is used to calculate the average crystallite size, or D. K is chosen in this case to be 0.94 in order to be consistent with spherical crystallites that have cubic symmetry. λ=1.5406 ″ is the wavelength of the radiation used for analysis, and βs is the peak's full width.

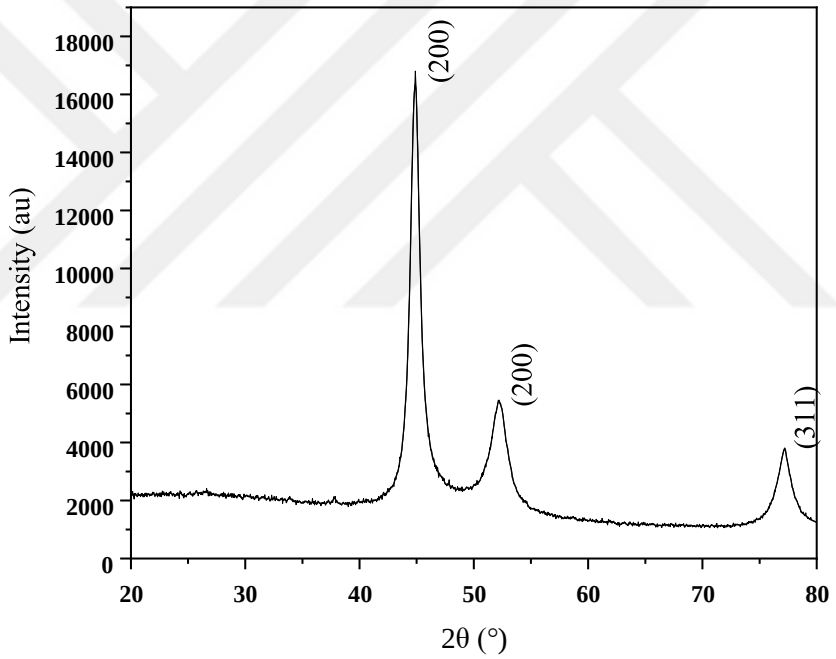

Figure 6: *XRD analysis of AuNP*

4.1.3 Scanning electron microscopy

Gold nanoparticles are uniformly dispersed, as shown by SEM analysis, supporting the stability of AuNP. The shape of the gold nanoparticles was spherical, with a variety of particle sizes ranging from 32 to 65 nm. SEM data suggest that the aggregation of smaller particles may be the cause of the larger gold particles seen in Figure 7.

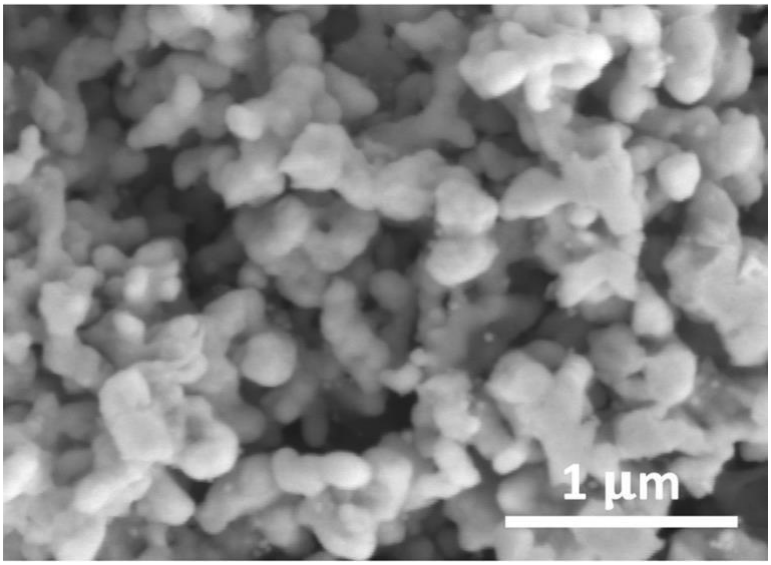

Figure 7: *SEM of AuNPs*

4.2 MTT Assay

The MTT reduction assay demonstrated a higher degree of sensitivity in assessing cytotoxicity following exposure to the investigated substances.

AuNPs demonstrated a concentration-dependent toxicity in SH-SY5Y cell line. Different concentrations of AuNPs were administered and when compared to control group, the toxicity of AuNPs increased with increasing concentrations. Specifically, 100 µg/µl AuNP showed the highest toxicity with a 25% cell survival (Figure 8, $p<0,05$*).

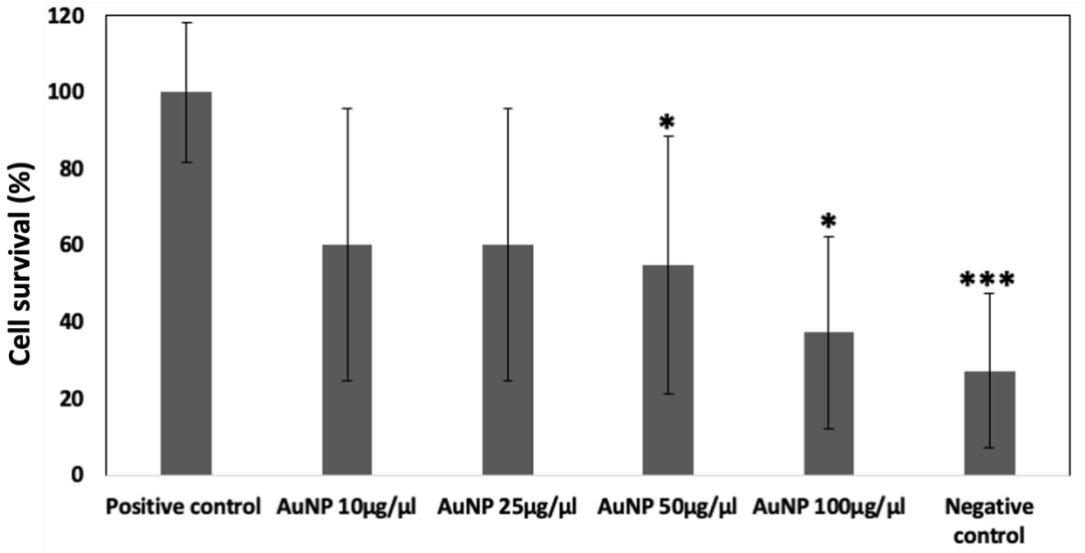

Figure 8: *Concentration-dependent cytotoxicity of AuNPs administered to SH-SY5Y cells (*p<0,05, ***p<0,001)*

4.3 RNA samples and qRT-PCR Analysis

The concentrations and A_{260}/A_{280} ratio of RNA samples isolated from SH-SY5Y cells are represented in Table 6. The values of A_{260}/A_{280} between 1.80 - 2.00 indicate the purity of RNA and the absence of DNA contamination.

Table 6
Concentrations and A_{260}/A_{280} ratio of RNA isolated from duplicate samples

RNA Sample	RNA concentration (ng/µl)	A_{260}/A_{280} ratio
Positive Control 1	1.991 ng/µl	2,00
Positive Control 2	921,4 ng/µl	2,01
AuNP treatment 1	2.351 ng/µl	1,96
AuNP treatment 2	2.297 ng/µl	1,97

The amplification and melt curve analysis of GAPDH and GSK3β are shown in figures 9 and 10, respectively. The melt curve analysis revealed that primers are binding the target sequence on cDNA template and there is no non-specific amplification. Moreover, non-template controls were not amplified and there were no peaks detected on melt curve analysis, suggesting the absence of primer-dimer formation.

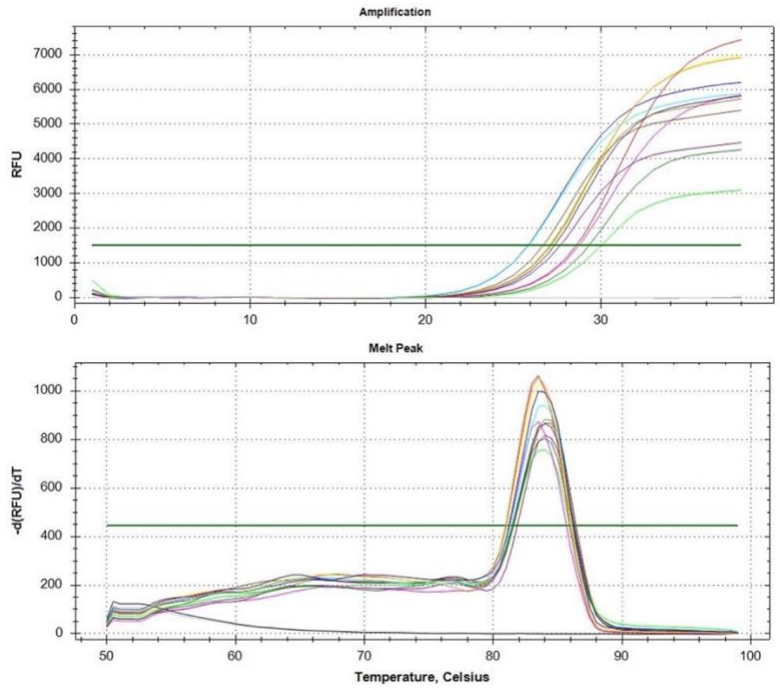

***Figure 9**: The amplification and melt curve analysis of qRT-PCR for GAPDH. All the samples give the peak approximately at 84°C.*

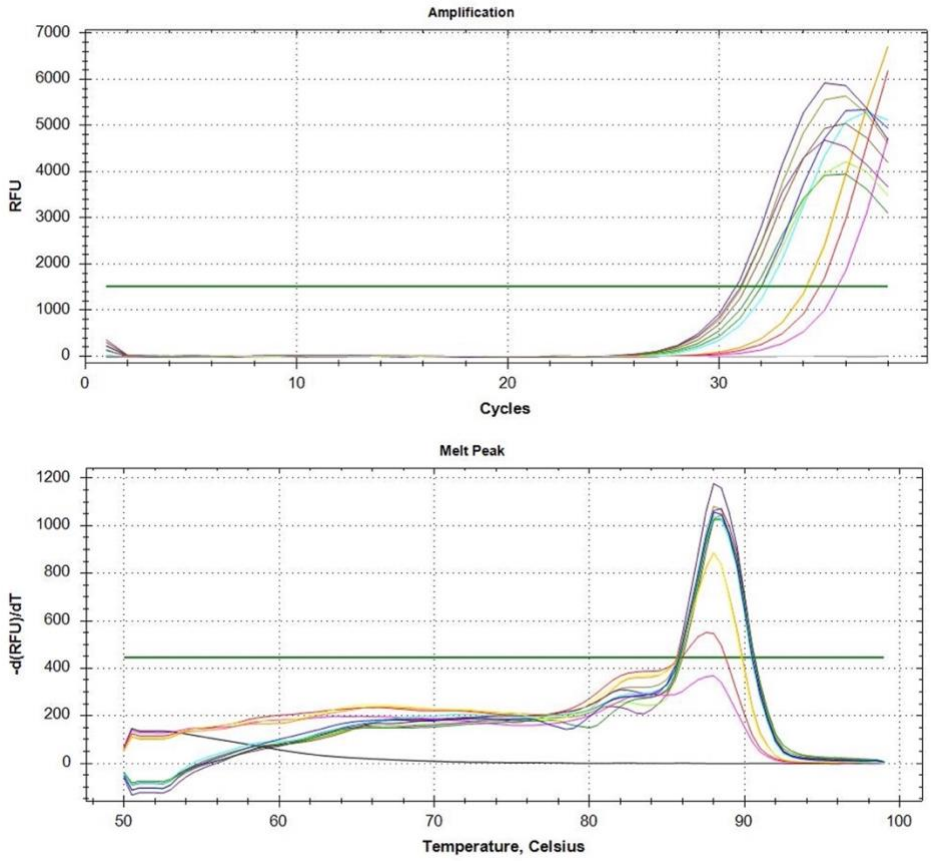

***Figure 10**: The amplification and melt curve analysis of qRT-PCR for GSK3β. All the samples give the peak approximately at 88°C.*

The calculation of the fold change was done as relative to the housekeeping gene, GAPDH, for AuNP treated group by using $2^{-\Delta\Delta Ct}$ method. The difference in the gene expressions are shown in Figure 11 as bar graphs. There is a statistically significant increase (*p<0,05) in the expression level of GSK3β in the AuNP administered groups when compared to the control group.

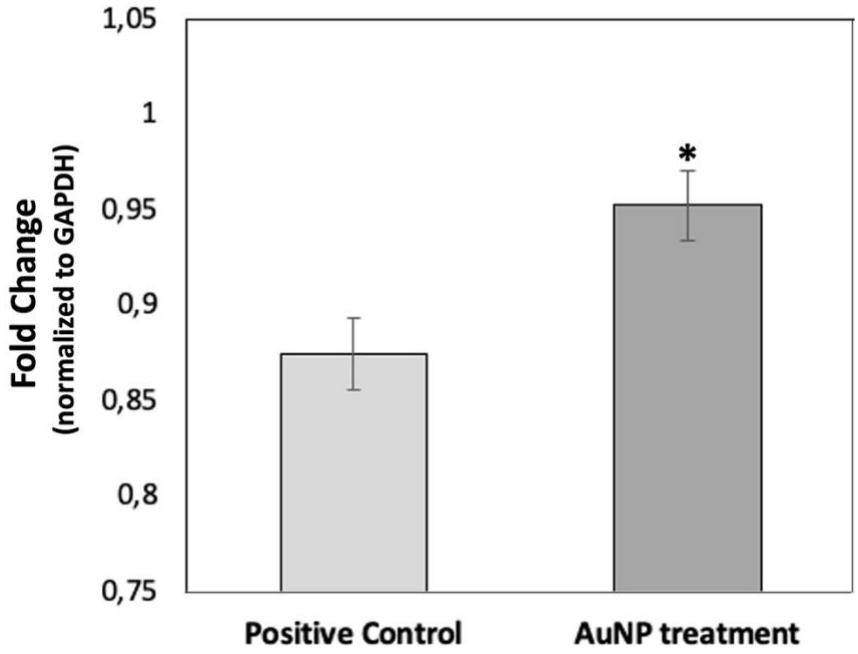

Figure 11: *GSK3β mRNA expression change with 10 µg/µl AuNP treatment to SH-SY5Y cells detected with qRT-PCR. AuNP administration resulted in an increase in the GSK3β expression (Positive Control: 0,87 ± 0,01; AuNP: 0,95 ± 0,01) (*p<0,05)*

Chapter 5
Discussion and Conclusion

5.1 Discussion

The size, the shape and the interaction between NPs and the molecules they are interacting in the solution are the main factors that make a significant impact on their optical properties. The measured solution features a surface Plasmon band that is easily visible and is characterized by a broad absorption peak centred at 564 nm. The prominent peak of AuNPs range from 500 to 600 nm in UV-vis spectrum.

AuNPs made with bay leaves were subjected to XRD analysis. At 2θ values of 44.8°, 52.1°, and 77.1°, there are several Bragg reflections that may be ascribed to the crystallographic planes (200), (200), and (311), in that order. The gold's face-centred cubic layout is in line with the previously described reflections. Expanding peaks in the data point to the possibility of nanoparticle formation.

The SEM method was used to observe the morphological characteristics of AuNPs. The examination demonstrated that the nanoparticles had a smooth surface and a nearly spherical shape. At a 500 nm magnification, the micrograph also showed that the powdered particles have a spherical shape with considerable aggregation within the size range of 50.3 nm.

Various concentrations of AuNPs were given to SH-SY5Y cells in order to evaluate their cytotoxicity and determine the ideal concentration. Different dosages were applied to the SH-SY5Y cells during the course of a 24-hour incubation period. In this investigation, the experimental concentrations used were 10, 25, 50, and 100 µg/µl. The MTT test was used to examine the impact of AuNPs on SH-SY5Y cells. A converging result was seen in the data from the concentrations of 10, 25, and 50 µg/µl. An estimated 25% decrease in cell viability was seen at a concentration of 100 µg/µl.

The concentration 10 µg/µl. of AuNPs was determined to be the least toxic one among all four concentrations tested by MTT. SH-SY5Y cells were treated with 10 µg/µl of AuNPs for RNA isolation. The purity and quality of RNA samples were determined by A_{260}/A_{280} ratio showing the absence of DNA contamination. The calculation of the fold change was done as relative to the housekeeping gene, GAPDH, for AuNP treated group by using $2^{\Delta\Delta Ct}$ method. The difference in the gene expressions was observed as

mentioned in figure 11 (Positive Control: 0,87 ± 0,01; AuNP: 0,95 ± 0,01*, $p < 0,05$). Similarly, it was also shown in the literature that intraperitoneal AuNP injections by using with 50 and 100 μg/kg of AuNPs-dexmedetomidine led to changes in GSK-3β protein and mRNA expressions, which were assessed by western blot and qRT-PCR, respectively. GSK-3β expression was demonstrated to increase in AuNP-dexmedetomidine administered groups relative to the control group. In the 100 μg/kg AuNP-dexmedetomidine group, there was a significant decrease in mRNA expression and an increase in GSK-3β protein expression ($p<0.05$). AuNPs-dexmedetomidine was suggested to modulate the GSK-3β signalling pathway to decrease the neurocognitive effect in rats under anaesthesia (Zhang et al.,2021).

5.2 Conclusion

AuNPS that been produced by green synthesis have been tested by many techniques such as UV-vis spectroscopy, XRD, and SEM. The results show a successful AuNP synthesis with average diameter between 32 to 65 nm and spherical morphology. Furthermore, the toxicity of the gold nanoparticle has been tested with MTT, and it was found that the increase of the concertation affects the cell viability and results in more toxicity. 10 μg/μl AuNP concentration was chosen as the least toxic concentration. It was shown that SH-SY5Y cells treated with 10 μg/μl AuNP had an increased GSK-3β mRNA expression. This finding is important since GSK-3β is a main factor of many diseases such as neuro-inflammatory diseases as well diabetes and cancer.

More research is needed to be done on the protein level to check if mRNA expression would also be reflected in protein level changes. Furthermore, AuNPs green-synthesis method needs to be further studied to increase the biocompatibility and to decrease the effect on GSK-3β gene expression. Last but not the least, GSK-3β-involved apoptotic pathways should be investigated upon AuNP exposure to be able to explain the toxic effect on SH-SY5Y cells.

REFERENCES

Adib Bin Rashid, "Utilization of Nanotechnology and Nanomaterials in Biodiesel Production and Property Enhancement", Journal of Nanomaterials, vol. 2023, Article ID 7054045, 14 pages, 2023. https://doi.org/10.1155/2023/7054045

Akhtar, K., Khan, S. A., Khan, S. B., & Asiri, A. M. (2018). Scanning electron microscopy: Principle and applications in nanomaterials characterization. *Handbook of materials characterization*, 113-145.

Baltzis, D., Pluquet, O., Papadakis, A. I., Kazemi, S., Qu, L. K., & Koromilas, A. E. (2007). The eIF2alpha kinases PERK and PKR activate glycogen synthase kinase 3 to promote the proteasomal degradation of p53. *The Journal of Biological Chemistry*, *282*(43), 31675–31687. https://doi.org/10.1074/JBC.M704491200

Bhat, R. V., Shanley, J., Correll, M. P., Fieles, W. E., Keith, R. A., Scott, C. W., & Lee, C. M. (2000). Regulation and localization of tyrosine216 phosphorylation of glycogen synthase kinase-3beta in cellular and animal models of neuronal degeneration. *Proceedings of the National Academy of Sciences of the United States of America*, *97*(20), 11074–11079. https://doi.org/10.1073/PNAS.190297597

Bilal, M., Barani, M., Sabir, F., Rahdar, A., & Kyzas, G. Z. (2020). Nanomaterials for the treatment and diagnosis of Alzheimer's disease: An overview. *NanoImpact*, *20*, 100251. https://doi.org/10.1016/J.IMPACT.2020.100251

CM de Lange, E. (2012). The physiological characteristics and transcytosis mechanisms of the blood-brain barrier (BBB). *Current Pharmaceutical Biotechnology*, *13*(12), 2319–2327. https://doi.org/10.2174/138920112803341860

Daneman, R. (2012). The blood-brain barrier in health and disease. *Annals of Neurology*, *72*(5), 648–672. https://doi.org/10.1002/ANA.23648

Daneman, R., & Prat, A. (2015). The Blood–Brain Barrier. *Cold Spring Harbor Perspectives in Biology*, *7*(1). https://doi.org/10.1101/CSHPERSPECT.A020412

dos Santos Tramontin, N., da Silva, S., Arruda, R., Ugioni, K. S., Canteiro, P. B., de Bem Silveira, G., Mendes, C., Silveira, P. C. L., & Muller, A. P. (2020). Gold Nanoparticles Treatment Reverses Brain Damage in Alzheimer's Disease Model. *Molecular Neurobiology*, *57*(2), 926–936. https://doi.org/10.1007/S12035-01901780-W

Draz, M. S., & Shafiee, H. (2018). Applications of gold nanoparticles in virus detection. *Theranostics*, *8*(7), 1985. https://doi.org/10.7150/THNO.23856

Elahi, N., Kamali, M., & Baghersad, M. H. (2018). Recent biomedical applications of gold nanoparticles: A review. *Talanta*, *184*, 537–556. https://doi.org/10.1016/J.TALANTA.2018.02.088

Grimes, C. A., & Jope, R. S. (2001). The multifaceted roles of glycogen synthase kinase 3beta in cellular signaling. *Progress in Neurobiology*, *65*(4), 391–426. https://doi.org/10.1016/S0301-0082(01)00011-9

Hammami, I., Alabdallah, N. M., jomaa, A. Al, & kamoun, M. (2021). Gold nanoparticles: Synthesis properties and applications. *Journal of King Saud University - Science*, *33*(7), 101560. https://doi.org/10.1016/J.JKSUS.2021.101560

Hartigan, J. A., & Johnson, G. V. W. (1999). Transient increases in intracellular calcium result in prolonged site-selective increases in Tau phosphorylation through a glycogen synthase kinase 3beta-dependent pathway. *The Journal of Biological Chemistry*, *274*(30), 21395–21401. https://doi.org/10.1074/JBC.274.30.21395

Hooper, C., Killick, R., & Lovestone, S. (2008). The GSK3 hypothesis of Alzheimer's disease. *Journal of Neurochemistry*, *104*(6), 1433–1439. https://doi.org/10.1111/J.1471-4159.2007.05194.X

Hu, X., Zhang, Y., Ding, T., Liu, J., & Zhao, H. (2020). Multifunctional Gold Nanoparticles: A Novel Nanomaterial for Various Medical Applications and Biological Activities. *Frontiers in Bioengineering and Biotechnology*, *8*, 556510. https://doi.org/10.3389/FBIOE.2020.00990/BIBTEX

Janzer, R. C., & Raff, M. C. (1987). Astrocytes induce blood-brain barrier properties in endothelial cells. *Nature*, *325*(6101), 253–257. https://doi.org/10.1038/325253A0

Kalimuthu, K., Cha, B. S., Kim, S., & Park, K. S. (2020). Eco-friendly synthesis and biomedical applications of gold nanoparticles: A review. *Microchemical Journal*, *152*, 104296. https://doi.org/10.1016/J.MICROC.2019.104296

Karthivashan, G., Ganesan, P., Park, S. Y., Kim, J. S., & Choi, D. K. (2018). Therapeutic strategies and nano-drug delivery applications in management of ageing Alzheimer's disease. *Drug Delivery*, *25*(1), 307–320. https://doi.org/10.1080/10717544.2018.1428243

Mikhailova EO. Green Synthesis of Platinum Nanoparticles for Biomedical Applications. J Funct Biomater. 2022 Nov 21;13(4):260. Doi: 10.3390/jfb13040260. PMID: 36412901; PMCID: PMC9680517.

Khan, A. K., Rashid, R., Murtaza, G., & Zahra, A. (2014). Gold nanoparticles: Synthesis and applications in drug delivery. *Tropical Journal of Pharmaceutical Research*, *13*(7), 1169–1177. https://doi.org/10.4314/TJPR.V13I7.23

Kong, F. Y., Zhang, J. W., Li, R. F., Wang, Z. X., Wang, W. J., & Wang, W. (2017). Unique Roles of Gold Nanoparticles in Drug Delivery, Targeting and Imaging Applications. *Molecules (Basel, Switzerland)*, *22*(9). https://doi.org/10.3390/MOLECULES22091445

Larsen, J., Martin, D., & Byrne, M. (2014). Recent advances in delivery through the blood-brain barrier. *Current Topics in Medicinal Chemistry*, *14*(9), 1148–1160. https://doi.org/10.2174/1568026614666140329230311

Leroy, K., & Brion, J. P. (1999). Developmental expression and localization of glycogen synthase kinase-3β in rat brain. *Journal of Chemical Neuroanatomy*, *16*(4), 279–293. https://doi.org/10.1016/S0891-0618(99)00012-5

Malik, S., Muhammad, K., & Waheed, Y. (2023). Emerging Applications of Nanotechnology in Healthcare and Medicine. *Molecules*, *28*(18), 6624. https://doi.org/10.3390/MOLECULES28186624

Meares, G. P., & Jope, R. S. (2007). Resolution of the nuclear localization mechanism of glycogen synthase kinase-3: functional effects in apoptosis. *The Journal of Biological Chemistry*, *282*(23), 16989–17001. https://doi.org/10.1074/JBC.M700610200

Moyaert, P., Padrela, B. E., Morgan, C. A., Petr, J., Versijpt, J., Barkhof, F., Jurkiewicz, M. T., Shao, X., Oyeniran, O., Manson, T., Wang, D. J. J., Günther, M., Achten, E., Mutsaerts, H. J. M. M., & Anazodo, U. C. (2023). Imaging bloodbrain barrier dysfunction: A state-of-the-art review from a clinical perspective. *Frontiers in Aging Neuroscience*, *15*.

Nanomaterials and Nanotechnology | Hindawi. (n.d.). Retrieved December 17, 2023

Phukan, S., Babu, V. S., Kannoji, A., Hariharan, R., & Balaji, V. N. (2010). GSK3β: role in therapeutic landscape and development of modulators. *British Journal of Pharmacology*, *160*(1), 1. https://doi.org/10.1111/J.1476-5381.2010.00661.X

Ramamurthy, C. H., Padma, M., mariya samadanam, I. D., Mareeswaran, R., Suyavaran, A., Kumar, M. S., Premkumar, K., & Thirunavukkarasu, C. (2013). The extra cellular synthesis of gold and silver nanoparticles and their free radical scavenging and antibacterial properties. *Colloids and Surfaces. B, Biointerfaces*, *102*, 808–815. https://doi.org/10.1016/J.COLSURFB.2012.09.025

Smijs, T. G., & Pavel, S. (2011). Titanium dioxide and zinc oxide nanoparticles in sunscreens: focus on their safety and effectiveness. *Nanotechnology, Science and Applications*, *4*(1), 95. https://doi.org/10.2147/NSA.S19419

Stewart, P. A., & Wiley, M. J. (1981). Developing nervous tissue induces formation of blood-brain barrier characteristics in invading endothelial cells: a study using quail--chick transplantation chimeras. *Developmental Biology*, *84*(1), 183–192. https://doi.org/10.1016/0012-1606(81)90382-1

Takahashi-Yanaga, F., Shiraishi, F., Hirata, M., Miwa, Y., Morimoto, S., & Sasaguri, T. (2004). Glycogen synthase kinase-3β is tyrosine-phosphorylated by MEK1 in human skin fibroblasts. *Biochemical and Biophysical Research Communications*, *316*(2), 411–415. https://doi.org/10.1016/j.bbrc.2004.02.061

Woodgett, J. R. (1990). Molecular cloning and expression of glycogen synthase kinase-3/factor A. *The EMBO Journal*, *9*(8), 2431–2438. https://doi.org/10.1002/J.1460-2075.1990.TB07419.X

Yamazaki, Y., & Kanekiyo, T. (2017). Blood-Brain Barrier Dysfunction and the Pathogenesis of Alzheimer's Disease. *International Journal of Molecular Sciences*, *18*(9). https://doi.org/10.3390/IJMS18091965

Yeh, Y. C., Creran, B., & Rotello, V. M. (2012). Gold Nanoparticles: Preparation, Properties, and Applications in Bionanotechnology. *Nanoscale*, *4*(6), 1871. https://doi.org/10.1039/C1NR11188D

Yusuf, A., Almotairy, A. R. Z., Henidi, H., Alshehri, O. Y., & Aldughaim, M. S. (2023). Nanoparticles as Drug Delivery Systems: A Review of the Implication of Nanoparticles' Physicochemical Properties on Responses in Biological Systems. *Polymers*, *15*(7). https://doi.org/10.3390/POLYM15071596

Zhang X, Xing Z, Li J, Tang S, Zhang Y. Gold Nanoparticles with Dexmedetomidine Regulate GSK-3*β* to Reduce Neurocognitive Effects in Anesthetized Rats. J Nanosci Nanotechnol. 2021 Dec 1;21(12):6205-6211. doi: 10.1166/jnn.2021.18745. PMID: 34229822.

Zhao, J., Xu, N., Yang, X., Ling, G., & Zhang, P. (2022). The roles of gold nanoparticles in the detection of amyloid-β peptide for Alzheimer's disease. *Colloid and Interface Science Communications*, *46*, 100579. https://doi.org/10.1016/J.COLCOM.2021.100579

Zlokovic, B. V. (2008). The blood-brain barrier in health and chronic neurodegenerative disorders. *Neuron*, *57*(2), 178–201. https://doi.org/10.1016/J.NEURON.2008.01.003